

NOTICE WARNING CONCERNING COPYRIGHT RESTRICTIONS:

The copyright law of the United States (title 17, U.S. Code) governs the making of photocopies or other reproductions of copyrighted material. Any copying of this document without permission of its author may be prohibited by law.

Discriminative MR Image Feature Analysis for
Automatic Schizophrenia and Alzheimer's
Disease Classification

Y. Liu, L. Teverovskiy and O. Carmichael, CMU
R. Kikinis and M. Shenton, Harvard Medical School
C. S. Carter, University of California, Davis
V. A. Stenger, S. Davis, H. Aizenstein,
J. T. Becker, O. L. Lopez and C. C. Meltzer, UPMC

CMU-RI-TR-04-152
The Robotics Institute
Carnegie Mellon University
Pittsburgh, PA 15213

©2004 Carnegie Mellon University

This work is partially supported by NIH grant R21 DA015900-01 and AG05133.

University Libraries
Carnegie Mellon University
Pittsburgh, PA 15213-3890

1 Introduction

Schizophrenia (SZ) is a severe, chronic and persistent mental disorder with onset in late adolescence or early adulthood resulting in lifelong mental, social and occupational disability. Alzheimer's Disease (AD) is a disease of aging, and the financial and social burdens of AD are compounded by recent and continued increases in the average life span. Assisting clinicians in making accurate early diagnostic distinctions becomes increasingly important with the development of effective treatments for CNS diseases.

Structural Magnetic Resonance (MR) images have an important advantage over other imaging modalities in that they are non-invasive and provide detailed information about gray and white matter parenchyma of the brain, and cerebrospinal fluid (CSF)-filled spaces. Classification of SZ and AD patients using high resolution MR Images of human brains is a challenging task even for the most experienced neuroradiologists. Many researchers are pursuing automatic or semi-automatic classification of patients based on MR images [2, 7, 15, 9, 17]. Most work has been done on precise segmentation of various anatomical structures for volumetric and local shape comparisons [15, 17]. Voxel-based approaches to the analysis of imaging data are powerful tools for rapid, automated comparisons of functional or structural imaging information in large numbers of subjects without the tediousness and subjective bias of hand tracing methods [1]. However, the validity of applying spatial normalization to image sets of elderly and AD brains has been challenged, and the greater variability in brain morphology that accompanies aging and dementia suggests that stereotactic anatomic standardization needs to be used with care [19]. In both cases of SZ and AD, there are considerable existing reported group morphological differences in specific anatomical structures of the brain [4, 19]. Due to group overlap, however, there is no existing reliable means to distinguish whether an individual MR image is from a specific disease category (SZ v. normal or AD v. normal), particularly in early stages of the disease. For example, several recent studies have suggested subtle population differences on MR images [5] of mild cognitive impairment (MCI) individuals, many of whom may go on to develop AD over the next several years. Indeed, those MCI subjects with smaller hippocampi had a greater likelihood of progressing to AD. Unfortunately, these findings have limited clinical utility for individual patients, as there is large overlap in hippocampal size between the groups due to high inter-individual variation of hippocampal volume with normal aging.

We propose an alternative image feature based statistical learning approach, in addition to anatomical structural morphology analysis, to better classify MR image classes. We formulate this as a supervised learning problem, where the MR image labels are given (class decisions are made by doctors based on specific clinical criteria for SZ and AD through behavior and cognitive

tests). The key element is to learn those MR image features that best discriminate disease classes. We shall examine both *separability* on the training data to explore, visualize and understand the structure of the data, and *generality* in terms of leave-one-out cross validation results to evaluate the generalization power of the selected MR image features.

Our method uses an ideal midsagittal plane based affine registration algorithm to bring all brain volumes into global spatial alignment. More than 3000 MR image features are extracted, which form a high dimensional coarse-to-fine hierarchical description of structural MR neuroimages, capturing quantified brain asymmetry, texture and statistical properties of MR images in corresponding local regions. Discriminative image feature subspaces are computed and screened. Our initial experimental results demonstrate an average of 88% classification accuracy on five binary classification setups (Tables 2 and 3). The outcome of our approach complements segmentation-based methods for enhanced automatic MR image classification. Such an automatic tool will aid in the diagnosis of neuropsychiatric disease, and potentially guide patient prognosis and therapy. The impact of such a computational framework may shift the emphasis from treating psychosis and preventing relapse towards illness prevention.

Section 2 gives a general description of our approach. Section 3 describes our experiments on SZ and AD datasets. We clarify some important issues in Section 4 and summarize the paper in section 5.

2 General Approach

We propose a novel approach for exploring thousands of image features to find a discriminative feature subspace where sample data points extracted from SZ or AD MR images are best separated from those of normal controls. The basic components in our computational framework include:

3D Image Alignment: All MR images for each classification problem in our feasibility study are taken using the same scanner and protocols. We verify image intensity consistency by carrying out an analysis of intensity histograms of input image sets from which no outliers are found.

All MR images are deformably registered using an affine registration algorithm based on maximization of mutual information [14]. For the schizophrenia study, we registered the images to a digital atlas provided by Dr. Kikinis' group at Harvard Medical School [11]. For the Alzheimer study we registered the images to the Montreal Neurological Institute (MNI) template [6]. The registration transformation is a global affine deformation, such that all brain images are normalized for shape and scale. Internal differences are intentionally **not** corrected by local deformations.

An automatic ideal midsagittal plane (iMSP) extraction algorithm [13] is applied to each 3D MR image before and after the above affine registration to (1) initialize yaw, roll angles and X-axis

translation [13] before the 3D registration for faster convergence and better registration accuracy. (2) validate iMSP accuracy after affine registration. Figure 1 shows some sample corresponding coronal slices of different subjects after affine registration, and (3) prepare each 3D image for iMSP based brain asymmetry image feature extraction.

Regions of Interest: Since each brain image is affinely registered with a digital atlas in 3D space, and resliced in the same way as the atlas, we are able to identify a region of interest (ROI) by specifying a stack of 2D slices on the atlas. In this initial work, only a portion of the 3D brain volume is used to test our algorithms. The 3D regions tested in this study are suggested by our medical collaborators. These are regions which may have potential relevance to disease classification on individual MR scans implied in the literature, though no definitive results have been reported.

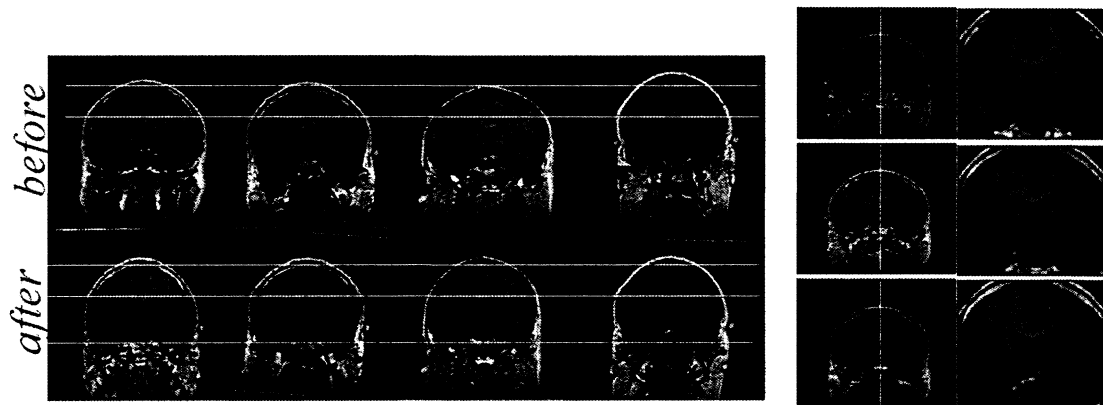


Figure 1: Left: sample corresponding slices from four different subjects, vertical correspondence indicated by yellow lines, before and after affine registration (left to right: control, schizophrenia patient (sz), control, sz). Note, the feature selection process also chooses which slices in a 3D volume is the most discriminative. Right: input consecutive slices of one subject where the iMSP is aligned with the center of the image in preparation for brain asymmetry computation, and the ROI is cropped uniformly on images from all subjects after registration.

Image Feature Types: Two general categories of image features are used in our feasibility study: (1) *statistical features* [10] (16 types) and *texture features* (25 types), a total of 41 image features are extracted (Figure 2). Table 1 lists the 41 image features used in this work.

The 25 *texture features* are Law's texture features [12]. 2D convolution kernels for texture discrimination are generated from a set of one-dimensional convolution kernels. From these one-dimensional convolution kernels, we can generate 25 different two-dimensional convolution ker-

Table 1: Statistical and Texture Features Definition

| | Statistical Features (16) | Texture Features (25) |
|----|---------------------------|---|
| 1 | mean intensity | <i>mnemonics</i> Five 1D convolution kernels Level L5 = [1 4 6 4 1] Edge E5 = [-1 -2 0 2 1] Spot S5 = [-1 0 2 0 -1] Wave W5 = [-1 2 0 -2 1] Ripple R5 = [1 -4 6 -4 1] |
| 2 | variance | |
| 3 | vertical edge | |
| 4 | horizontal edge | |
| 5 | diagonal edge | |
| 6 | (other) diagonal edge | |
| 7 | edge orientation | |
| 8 | standard deviation | Twenty-Five 2D convolution kernels |
| 9 | maximum intensity | |
| 10 | minimum intensity | |
| 11 | median intensity | |
| 12 | intensity range | |
| 13 | energy | |
| 14 | skewness | |
| 15 | kurtosis | |
| 16 | entropy | |

nels by convolving a *vertical* 1-D kernel with a *horizontal* 1D kernel. As an example, the L5E5 kernel is found by convolving a vertical L5 kernel with a horizontal E5 kernel.

Figure 2 shows some of the extracted features on a 2D coronal slice. For each filtered brain slice $I(x, y)$, we also compute an *asymmetry brain* image feature defined as: $D(x, y) = I(x, y) - I_{vRef}(x, y)$ where I_{vRef} is the vertical reflection of the original feature image $I(x, y)$. Since $I(x, y)$ is already centered by the iMSP, $D(x, y)$ is the intensity difference of the corresponding left and right halves of a brain slice.

Image Feature Location: One important aspect of our exploration is to localize where the potential discriminative features lie in the ROI. We subdivide each slice of the registered brain (in coronal or axial direction) hierarchically. Figure 3 shows such a division on three levels (each level has 1, 4 and 16 regions respectively). For each level, we compute (1) mean and (2) variance of the image feature in each subdivision. Given both original image feature slices and bilateral asymmetry difference slices, a total of $(1+4+16)*4 = 84$ “location features” are generated for each image feature type on each 2D slice. Therefore we have a total of $41 \times 84 \times \#of\ slices = 3444 \times \#of\ slices$

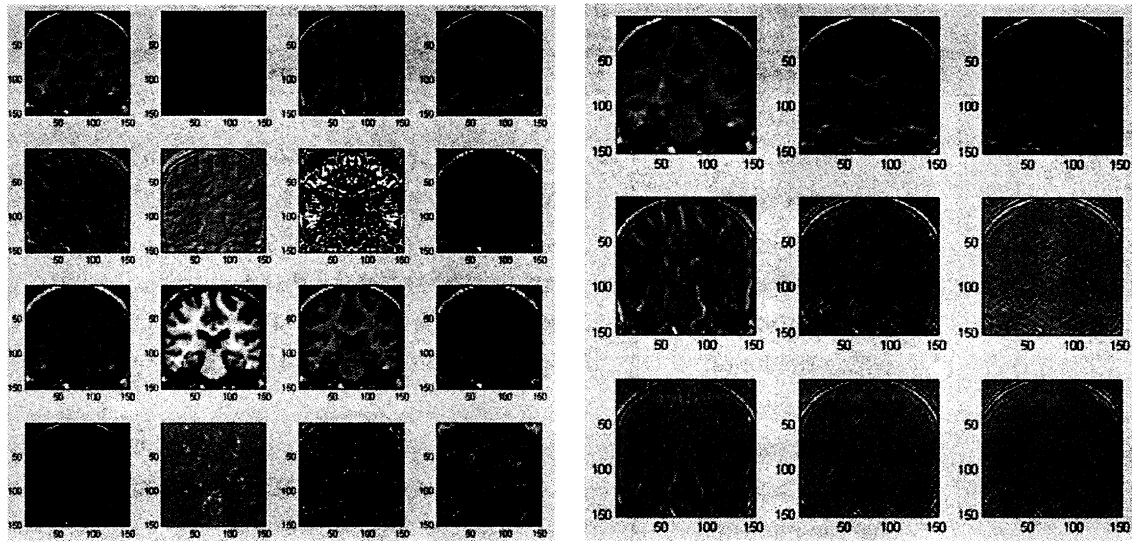


Figure 2: Left: A sample view of all extracted statistical features. From left to right, top to bottom: mean intensity, variance, vertical edge, horizontal edge, diagonal edge, (other) diagonal edge, edge orientation, standard deviation, maximum intensity, minimum intensity, median intensity, range, energy, skewness, kurtosis, entropy. Right: the top-left 3 by 3 2D texture features out of the 25 Law's texture features: L5L5, E5L5, S5L5, W5L5, R5L5; L5E5, E5E5, S5E5, W5E5, R5E5; L5S5, E5S5, S5S5, W5S5, R5S5. They are formed by five 1D convolution kernels: Level, L5 = [1 4 6 4 1]; Edge, E5 = [-1 -2 0 2 1]; Spot, S5 = [-1 0 2 0 -1]; Wave, W5 = [-1 2 0 -2 1]; and Ripple, R5 = [1 -4 6 -4 1].

dimensional feature space with both regional, statistical and textural information to explore.

Discriminative Feature Evaluation and Screening: A common theme in our research is to use available image features selectively for different image discrimination tasks; this is especially effective when there is redundancy within different feature dimensions which is a strong characteristic of image features. For a feature F with values S_F in a data set with C total classes, we define an *augmented variance ratio* (AVR) as follows

$$AVR(F) = \frac{Var(S_F)}{\frac{1}{C} \sum_{i=1..C} \frac{Var_i(S_F)}{\min_{i \neq j} (|mean_i(S_F) - mean_j(S_F)|)}}$$

where $Var_k(S_F)$ is the variance of the subset of values from feature F which belongs to class c and $mean_i(F)$ is the mean of feature F 's values in class i . AVR is the ratio of the variance of the feature between subjects to the variance of the feature within subjects, with an added penalty for features that have close inter-subject mean values. Individual features that have higher variance

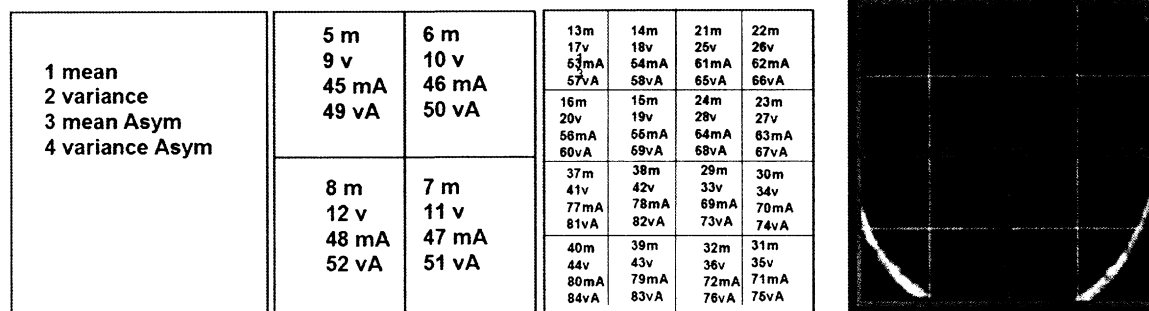


Figure 3: This diagram illustrates the hierarchical decomposition of each slice. For each image feature we compute the mean (m), variance (v), asymmetry mean (mA), and asymmetry variance (vA) in each red, green, and yellow block indicated (right). We then concatenate all of these local measures into a feature vector. The numbers in each block indicate an index of the feature location (clockwise rotation of the four quarters starting from top-left).

ratios are more discriminative. AVR ranked features provide us with a quantitatively plausible approach to remove non-discriminative features before applying forward sequential feature subset selection [3]. Feature subset selection is carried out using Linear Discriminant Analysis (LDA) [8] as the evaluation classifier, which has a measure for discriminating power that is consistent with AVR.

Separability Analysis: We define *separability* of a data set in a particular feature subspace as the classification rate (plus sensitivity and specificity) in that feature space using a K-nearest neighbor (KNN) classifier [8] with a fixed K. Different feature subspaces are explored using either an exhaustive search for all triplet features or a forward sequential selection method [3]. The result is a set of image feature subspaces with the highest classification rates indicating highest degrees of separation among image classes.

Prediction: Given N data points (3D MR images from N different subjects), $N - 1$ are used for training to find discriminative feature subspaces, and the one left out is used as the unseen test sample for the classifier prediction accuracy evaluation. This process is repeated N times in a round-robin manner. Summarize the classification results on each of the N subjects during the leave-one-out (LOO) cross validation, we compute the LOO classification rate, sensitivity and specificity.

3 Experiments

3.1 Classification of Schizophrenia Patients

A feasibility study is carried out using (1) an image data set from Dr. Shenton of Harvard medical school [18] containing MR images of 15 schizophrenia patients (chronical) and 15 controls; and (2) an image data set from Univeristy of Pittsburgh containing MR images of 24 first episode (FE) schizophrenia patients and 27 normal controls. The controls are matched in age, family background and handedness. From each 3D MR scan a set of 2D coronal slices are sampled around the region of interest (Figure 1). Taking the top 30 most discriminative features from more than 3000 candidates, followed by sequential forward feature selection using LDA [3], and LOO using KNN we achieve the results listed in Table 2.

Table 2: Schizophrenia Classification Experimental Results

| Disease Class # of Subjects | CTL v. SZ (chronical) (15 v. 15 from Harvard) | CTL v. SZ (first episode) (27 v. 24 from UPMC) |
|--------------------------------|--|---|
| Separability | 100% | 90% |
| Sensitivity | 100% | 88% |
| Specificity | 100% | 92% |
| Prediction (LOO) | | |
| Classification Rate | 90% | 78% |
| Sensitivity | 93% | 79% |
| Specificity | 87% | 77% |

Figure 4 shows two image feature subspaces automatically selected from the Harvard schizophrenia data. Clear linear separation between SZ patients and controls is observed. The locations of selected discriminative features include quantified brain asymmetry from temporal lobe regions, which echos previous findings on temporal lobe asymmetry difference between normal and schizophrenia patients [18].

3.2 Classification of Alzheimer's Disease

A set of 60 subjects are selected by experts from University of Pittsburgh Alzheimer's Disease Research Center (ADRC funded by NIH), in which 20 are normal controls, 20 are subjects with MCI, and 20 are diagnosed AD patients matched on age, education and sex.

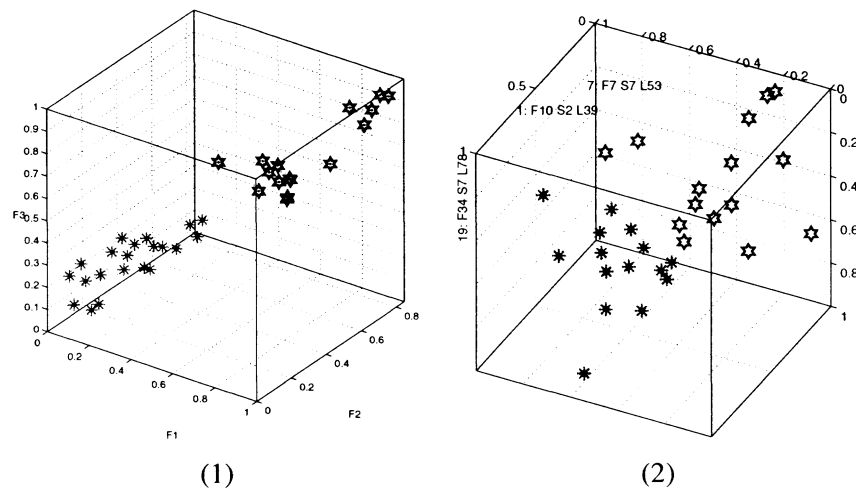


Figure 4: Two 3-feature subspaces automatically selected for two different schizophrenia MR image data sets. (1) Harvard image set of chronic SZ versus normal controls. (2) UPMC image data set of FE SZ patients versus normal controls. In both cases, clear linear class separation can be observed where red stars are from schizophrenia MR images and blue hexagons are from normal controls. The three feature dimensions in (1) correspond to range feature in lower left quarter, L5E5 texture feature in top-middle-left block and horizontal edge filtered from the lower left quarter (Figure 3). In (2) the three features are from slice 2, statistical feature 10, location 39; slice 7, statistical feature 7, location 53, and slice 7, texture feature 18 at location 78 (local region brain asymmetry).

The image data are acquired in three dimensions to obtain 120 thin, contiguous images throughout the entire brain. The contrast was designed to maximize the gray-white matter and CSF differences (TR=25, TE=5, slices = 1.5mm, 0 gap, 40 degrees flip angle, FOV=24x18cm), the data are gathered in the coronal plane, this minimizes partial voluming effects. See Table 3 for classification results on this data set. Figure 6 shows statistics of selected discriminative image features for MCI versus controls. These plots indicate the most frequently selected image features and brain regions.

Combination of Image Features with Shape Features: Using LONI (Laboratory of Neuroimaging, UCLA) software [16], we have hand-segmented hippocampi for each subject in the 20-20-20 (control, MCI and AD) image data set. We explore the effect of adding this morphology information into our image feature selection process. Several shape features are computed using the hand traced 3D surface information. They are: hippocampus volume, the coordinate of the centroid of the hippocampus, the x,y, and z dimensions of the bounding box around the hippocampus, the 2nd-

Table 3: Alzheimer’s Disease Classification Results

| Disease Class | CTL v. MCI | CTL v. AD | MCI v. AD | MCI v. AD |
|---------------------------|------------|-----------|-----------|--------------------|
| # of Subjects | 20 v. 20 | 20 v. 20 | 20 v. 20 | 20 v. 20 |
| Features Used | Image | Image | Image | Image+Shape |
| Separability | 100% | 96% | 97% | 98% |
| Sensitivity | 100% | 95% | 100% | 100% |
| Specificity | 100% | 96% | 95% | 95% |
| LOO Classification | 93% | 93% | 78% | 88% |
| Sensitivity | 100% | 85% | 80% | 85% |
| Specificity | 85% | 100% | 75% | 90% |

order geometric moments of the hippocampus along three axes, and 2nd-order legendre moments of the hippocampus. Adding these shape features to the image feature selection process we have achieved better classification rates. For MCI versus AD case, for example, the right hippocampus volume and second-order geometric moments along the XZ direction respectively are selected jointly with image features with improved separability and LOO results (right-most column in Table 3). This result indicates that the image intensity features and shape features complement each other in discriminative power for disease classification.

Experiments with Multiple Classifiers: We have also experimented with many standard classifiers including decision trees, decision graphs, decision stumps, instance-based learning, naive bayes and support vector machines (SVM) with or without bagging or stacking on the top 100 AVR ranked image features. We found the performance depends primarily on the features used. Using the top 30 AVR ranked image features in combination with shape features, for example, decision stumps achieves the best classification rates for control versus AD, 90% (sensitivity and specificity).

4 Discussion

Our method establishes a framework for a computer system to automatically explore very high dimensional image feature spaces in search of a discriminative subspace. The preliminary results suggest that regional image features contain highly discriminative information to separate different CNS diseases from normal brains on several limited (15 to 27 subjects in each disease class) but well-chosen image sets. The leave-one-out results also suggests the potential to build a disease

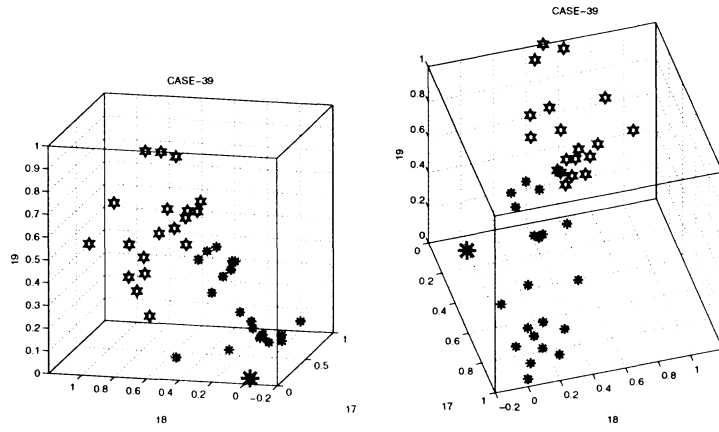


Figure 5: Sample LOO result showing the predicting power of the learned image feature space for MCIs versus normal controls. The large star indicates the subject (an MCI patient) which is left out as the testing sample, as it is placed back into the learned discriminative feature subspace for classification. In this case, the classification result is positive. The three feature axes are all from slice one (Figure 6): 17 is the mean of bilateral asymmetry value from region 64 when image feature median intensity is used. 18 is the same as 17 except it is from image feature mean intensity, and 19 is from region 27 representing the variance of a texture feature combining *spot* and *ripple* (Figure 3).

predictor that uses critically chosen image features to classify an unknown image into one of the correct disease categories with probability much higher than chance. In the case of AD, for example, the LOO result of controls versus AD surpasses the result reported in [9], which is based on only one-time division of the input data — the probability of chance is high. Our result, on the other hand, is based upon a statistically justified 40-way division LOO cross validation [8]. Using selected triplet image features alone on SZ classification, our result (Table 2) also surpasses the performance reported in [17] on the same image set.

One non-intuitive aspect of our approach perhaps lies in the fact that, contrary to most medical image analysis work and particularly in SZ and AD MR image studies, no anatomical segmentation of the MR neuroimages is carried out. Instead, we bring all brain images into a common coordinate system where their iMSPs coincide, divide each 2D slice into equal sized geometric regions and compute image properties in that region where the true anatomical structures in corresponding patches may or may not correspond. Our method takes advantage of this local non-correspondence or intensity discrepancy by examining quantitatively whether it is representative of its own image semantic class (disease). Another advantage of our method over, e.g. neural network approaches, is that it is not a black-box. We are able to visualize the relative weights in the found discrimina-

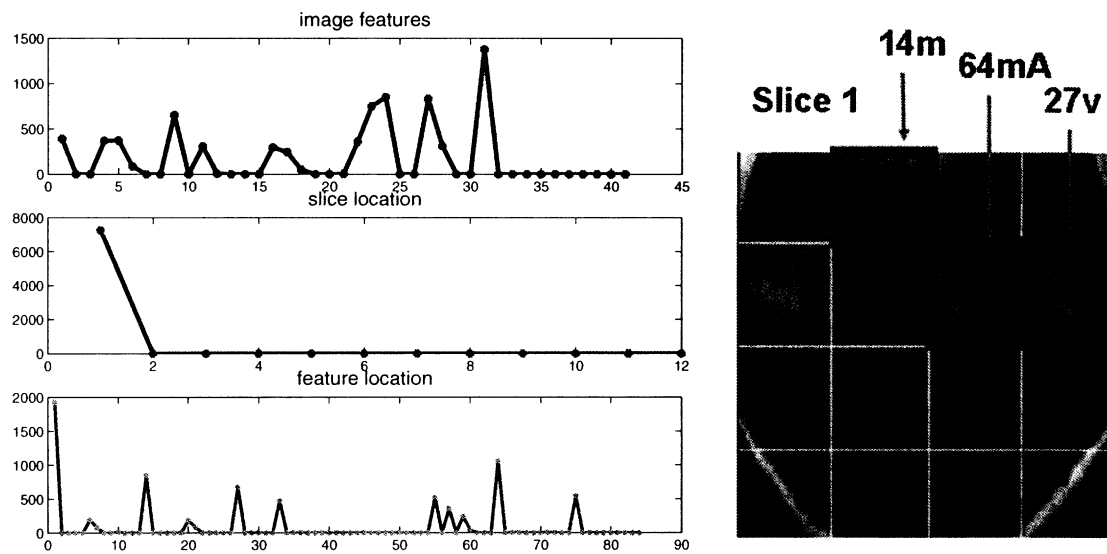


Figure 6: Three plots showing feature type, slice number and geometric location of the most discriminative features selected for MCI versus normal controls prediction. Top: The most popular image feature is the 15th texture feature (31st on the X axis) composed of ripple and spot. Middle: The most important slice in a 3D image is the most inferior slice in the chosen ROI. Bottom: besides the feature extracted from location 1 (overall mean), the top three most discriminative features come from region 64 (mean intensity asymmetry value), region 14 (mean value of the top left-middle region) and region 27 (the intensity variance) (Figure 3).

tive subspace, data points distributions, and trace back the type and the (anatomical) locations of selected image features (Figure 6).

There are several limitations in our current experiment setup, including: (1) the data set is small. (2) the skull is not removed from the image beforehand such that some boundary regions contain background signal intensity. (3) image features are all 2D features extracted from each slice. Therefore we propose to gather more MR image cases, improve image preprocessing and add a large variety of image feature extractors, especially 3D image features in our future research.

5 Conclusion

In this paper, we propose and validate a new method for SZ and AD MR image discrimination via exploration in high dimensional image feature spaces. For a given disease versus control data

set and a local ROI, the algorithm is able to automatically find both the type and the location of the most discriminative image feature subsets for data visualization, exploration and prediction. In these subspaces the two classes can be linearly separated. Based on clinical need, we have introduced an intermediate disease category, first episode for SZ and MCI for AD, forming a more challenging classification problem. Our classification algorithm has shown superior performance compared with existing reported results. Furthermore, the learned feature subspace is stable as demonstrated by the results of leave-one-out cross validation. The locations of discriminative image features found in focused ROIs are clinically relevant, and include quantified brain asymmetry, which echos previous findings on temporal lobe asymmetry in SZ and hippocampi asymmetry in AD patients. We plan to explore the whole brain systematically in future studies, and test our method on a larger, well defined data set.

References

- [1] J. Ashburner and K.J. Friston. Voxel-based morphometry—the methods. *Neuroimage*, 11(6 Pt 1):805–21, 2000.
- [2] R.M. Bilder, H. Wu, B. Bogerts, M. Ashtari, D. Robinson, M. Woerner, J.A. Lieberman, and G. Degreef. Cerebral volume asymmetries in schizophrenia and mood disorders: a quantitative magnetic resonance imaging study. *International Journal of Psychophysiology*, 34(3):197–205, December 1999.
- [3] C. M. Bishop. *Neural Networks for Pattern Recognition*. Clarendon Press, 1995. ISBN:0198538499.
- [4] R.W. Buchanan, K. Vldar, P.E. Barta, and G.D. Pearlson. Structural evaluation of the pre-frontal cortex in schizophrenia. *American Journal of Psychiatry*, 155:1049–55, 1998.
- [5] G. Chetelat and J. C. Baron. Early diagnosis of alzheimer’s disease: contribution of structural neuroimaging. *Neuroimage*, 18(2):525–541, March 2003.
- [6] D. L. Collins, A. Zijdenbos, V. Kollokian, J. G. Sled, N. J. Kabani, C. J. Holmes, and A. C. Evans. Design and construction of a realistic digital brain phantom. *IEEE Trans. Med. Imag.*, 17:463–468, 1998.
- [7] T.J. Crow. Schizophrenia as an anomaly of cerebral asymmetry. In K. Maurer, editor, *Imaging of the brain in psychiatry and related fields*. Springer-Verlag, 1993.
- [8] R.O. Duda, P.E. Hart, and D.G. Stork. *Pattern Classification*. John Wiley & Sons, New York, 2001.
- [9] P.A. Freeborough and N. C. Fox. MR image texture analysis applied to the diagnosis and tracking of alzheimer’s disease. *IEEE Transactions on Medical Imaging*, 17(3):475–479, June 1998.
- [10] A. Jain, R.P.W. Duin, and J. Mao. Statistical pattern recognition: a review. *IEEE Trans. Pattern Analysis and Machine Intelligence*, 22(1):4–37, Jan. 2000.
- [11] R. Kikinis, M.E. Shenton, D.V. Iosifescu, R.W. McCarley, P. Saiviroonporn, H.H. Hokama, A. Robatino, D. Metcalf, C.G. Wible, C.M. Portas, R.M. Donnino, and F.A. Jolesz. A digital brain atlas for surgical planning, model-driven segmentation, and teaching. *IEEE Transactions on visualization and computer graphics*, 2(3):232–240, September 1996.

- [12] K. Law. *Textured Image Segmentation*. PhD thesis, University of Southern California, January 1980.
- [13] Y. Liu, R.T. Collins, and W.E. Rothfus. Robust Midsagittal Plane Extraction from Normal and Pathological 3D Neuroradiology Images. *IEEE Transactions on Medical Imaging*, 20(3):175–192, March 2001.
- [14] F. Maes, A. Collignon, D. Vandermeulen, G. Marchal, and P. Suetens. Multimodality image registration by maximization of mutual information. *IEEE Transactions on Medical Imaging*, 16(2):187,198, 1997.
- [15] R.W. McCarley, C.G. Wible, Y.H. Frumin, J.J. Levitt, I.A. Fischer, and M.E. Shenton. MRI anatomy of schizophrenia. *Society of Biological Psychiatry*, 45:1099–1119, 1999.
- [16] D.E. Rex, J.Q. Ma, and A.W. Toga. The LONI pipeline processing environment. *Neuroimage*, 19(3):1033–48, 2003.
- [17] M.E. Shenton, G. Gerig, R.W. McCarley, G. Szekely, and R. Kikinis. Amygdala-hippocampal shape differences in schizophrenia: the application of 3d shape models to volumetric mr data. *Psychiatry Research Neuroimaging*, 115:15–35, 2002.
- [18] M.E. Shenton, R. Kikinis, F.A. Jolesz, S.D. Pollak, M. Lemay, C.G. Wible, H. Hokama, J. Martin, B.S.D. Metcalf, M. Coleman, M. A. Robert, and T.W. McCarley. Abnormalities of the left temporal lobe in schizophrenia. response to roth, pfefferbaum and to klimke and knecht. *New England Journal of Medicine*, 327(SPL Technical Report 3):75–84, 1992.
- [19] P.M. Thompson, D. MacDonald, M.S. Mega, C.J. Holmes, A.C. Evans, and A.W. Toga. Detection and mapping of abnormal brain structure with a probabilistic atlas of cortical surfaces. *Journal of Computer Assisted Tomography*, 21(4):567–81, 1997.

